Reig Cerdá, L.; Soriano Martinez, L.; Borrachero Rosado, MV.; Monzó Balbuena, JM.; Paya Bernabeu, JJ. (2014). Influence of the activator concentration and calcium hydroxide addition on the properties of alkali-activated porcelain stoneware. Construction and Building Materials. 63:214-222. doi:10.1016/j.conbuildmat.2014.04.023.

Influence of the activator concentration and calcium hydroxide addition on the properties of alkali-activated porcelain stoneware

L. Reig [a], L. Soriano [b], M.V. Borrachero [b], J. Monzó [b], J.Payá [b]

[a] EMC, Universitat Jaume I, Av. Sos Baynat s/n 12071 Castelló de la Plana, Spain.

[b] Instituto de Ciencia y Tecnología del Hormigón (ICITECH), Universitat Politècnica de València, Camino de Vera s/n 46022 Valencia, Spain.

Corresponding author: L. Reig; lreig@uji.es

Tel.: +34 964 729163 / Fax: +34 964 728106

E-mail address: lreig@uji.es; lousomar@gmail.com; vborrachero@cst.upv.es; jmmonzo@cst.upv.es; jjpaya@cst.upv.es

Abstract

Porcelain stoneware tiles are produced in large quantities in Spain. The aim of this research was to investigate the influence of the alkali activator concentration and calcium dosage on the fresh behavior, compressive strength and microstructure of the binder produced by the alkali activation of porcelain stoneware waste. The results show that the activator concentration strongly influences the fresh behavior of mortars. The calcium to sodium molar ratio (M_{Ca}) greatly influenced the hardening process so that the mortars mixed with a constant M_{Ca} ratio exhibited similar setting times. Furthermore, when keeping the SiO_2 concentration constant, a linear evolution of compressive strength with sodium addition was observed. Mortar samples with up to 36 MPa under compression were obtained after curing for 7 days at 65°C.

Keywords: Ceramic waste (D), Waste Management (E), Alkali-Activated Cement (D), Compressive Strength (C).

1. Introduction

Manufacturing Portland cement (OPC) is a resource-exhausting, energy-intensive process that releases huge amounts of greenhouse gas CO_2 into the atmosphere. Indeed, the production of 1 ton of Portland cement requires about 2.8 tons of raw materials, including fuel and other constituents [1]. Efforts have been made by the scientific community and the OPC industry to reduce this impact. Among the different alternatives proposed, alkali-activated cementitious materials, produced from an alumino-silicate precursor activated in a high alkali solution, have attracted increasing attention as a viable solution to reuse and recycle industrial solid wastes and by-products [2]. When compared to Portland cement, the mortar and concrete made from the alkali activation process has its advantages, such as higher strength (when properly designed), low cost, excellent durability, low energy consumption and reduced greenhouse gas emissions [3-5]. Furthermore, one of the most advantageous aspects it offers is that it allows the development of binders to be made entirely, or almost entirely, from waste materials [6].

Generally, materials containing amorphous silica and alumina can be activated by alkalis. As reviewed by Li et al. [5], two models have been established for alkali-activated binding systems. The first is the case of blast furnace slag activation (GGBFS, Si+Ca) with mild alkaline solutions, where calcium silicate hydrate is the main reaction product. The general example for the second alkali activation model is metakaolin (MK) or Class F fly ash, (Si+Al), with medium to high alkaline solutions, giving rise to zeolite-like geopolymers. The stages that take place to form the alkaline silico aluminate network in the latter system are summarized in [7,8]. Initially, the dissolution of solid species occurs, and the OH^- ions in the alkaline medium sever the covalent Si–O–Si, Si–O–Al and Al–O–Al bonds present in the amorphous phase of the solid material. Silicon and aluminum ions are released into the medium, where they form Si–OH and Al–OH groups. This stage is followed by the reorganization and formation of small nuclei that later polycondensate to form an alkaline aluminosilicate gel characterized by its three-dimensional structure. As pointed out by Yip et al. [9], the main difference between the hydration product from GGBFS activation (Case 1) and that from fly ash activation (Case 2) is calcium. Although this element is not essential in any part of a basic geopolymeric structure, it is generally accepted that if sufficient calcium is added to the system, a C-(A)-S-H or (C,N)-A-S-H-based cementitious material may form instead [10-12]. This fact was proved by Alonso and Palomo [7], who mixed highly pure

metakaolin with different $Ca(OH)_2$ solid contents (30-50%). Although the main reaction product of alkaline activation is an amorphous aluminosilicate with a tridimensional network and cementitious properties, addition of calcium hydroxide to the system has been found to provoke the formation of a C-S-H gel type as a secondary reaction product [7]. Moreover, several studies have shown that the addition of moderate amounts of calcium has a positive effect on the mechanical properties of alkali-activated binders [9,10,13].

A large number of minerals and by-products have been alkali-activated, of which metakaolin [7,13,14], fly ash [1,8,15,16] and ground granulated blast furnace slag [5] have been the most extensively analyzed. Increasing interest in the alkali activation process has led the scientific community to identify other suitable waste materials for the alkali activation process. Among the experimental research performed, Lee et al. [17] combined three different industrial by-products (fly ash, slag and bottom ash) to develop a new low-strength material using NaOH as an activator. He et al. [2] also combined rice husk ash with the major waste by-product that originates when extracting alumina from bauxite ores (red mud) to develop alkali-activated pastes with compressive strengths of up to 20.5 MPa after 49 curing days (room temperature). In the work by Yusuf et al. [18], 28-day compressive strength values of 44 MPa were achieved through the activation of palm oil fuel ash and ground blast-furnace slag combinations with sodium silicate and sodium hydroxide. In the study by Kourti et al. [19], air pollution control residues and glass-forming additives were mixed to obtain a glass using DC plasma technology. High compressive strengths (~130 MPa) were achieved by the alkali activation of this high calcium alumino-silicate glass with a sodium hydroxide solution. Similarly, Sun et al. [20] reported high compressive strength values (a maximum of 71.1 MPa in samples cured for 28 days) and good high-temperature properties (higher strength after heat treatment of 1000°C) in ceramic waste activated with alkali hydroxides and sodium/potassium silicate solutions. Ceramic materials were also activated in the work by Khater et al. [21], where 23 MPa were achieved under compression in pastes developed by the alkali activation of concrete and demolished walls after 90 days of curing at 40ºC. Hydrated-carbonated Portland cement was also activated by Payá et al. [4], where mortars with compressive strengths over 10 MPa were obtained after curing at 65°C for 3 days.

Different types of ceramic tiles [22,23] have also been successfully activated using NaOH and sodium silicate solutions. These products are widely used in construction in Spain and, despite the Spanish production rate having lowered by almost 40% from 2006 to 2010 (608 and 366 million m^2, respectively), it still ranked seventh in 2010, with 3.8% of the total world production [24]. As explained by Puertas et al. [25], although ceramic tiles can be reused for the tile manufacturing process, the cost of the milling required for that purpose is not compensated by the savings generated in raw materials. Ceramic materials have also been used as cement admixtures [25,26] and concrete aggregates [27]. However, only a portion (usually 10-35%) of cement is replaced in these applications.

In the work by Reig et al. [23], porcelain stoneware tile (PS) wastes were activated, and mortars with compressive strengths close to 30 MPa were obtained after 7 curing days at 65ºC. Similarly to the previous work by Granizo et al. [13], which analyzed the structure of metakaolin and $Ca(OH)_2$ mixes (1:1), a major influence of $Ca(OH)_2$ addition was noticed in [23]. So, while no activation took place in the absence of calcium hydroxide, rapid setting occurred when 5% of PS was replaced with this material. However, no correlation between the rapid setting of mortars and alkaline concentration or calcium addition was observed.

The study discussed herein is actually a logical extension of the previous work presented in [23], and it aims to understand the influence of the alkali activator concentration and calcium dosage on the fresh behavior and properties of the hardened binder developed by the alkali activation process.

2. Experimental

2.1. Materials

Porcelain stoneware (PS) tiles were broken with a hammer, crushed in a jaw crusher (BB200, Retsch) and dry milled in alumina media for 30 minutes. Calcium hydroxide (93% purity) was used as a partial replacement of ceramic waste. Sodium hydroxide pellets (98% purity, Panreac), water and sodium silicate (Merck, SiO_2=28%, Na_2O=8%, H_2O=64%) were used to prepare alkali-activating solutions.

After the milling process, dense irregular particles were obtained. The mean particle diameter, determined through laser granulometry (Mastersizer 2000, by Malvern instruments), was close to 21 μm, with a d_{90} of 53 μm (90 vol.-% with this size). The chemical composition, determined by X-ray fluorescence (XRF), was similar to that presented by metakaolin [5], with SiO_2 (71 wt-%) and Al_2O_3 (19.3 wt-%) being the major constituents. The other components, such as Na_2O (4.7 wt-%), CaO (0.5 wt-%) or Fe_2O_3 (1.1 wt-%), were not significantly detected.

The amorphous content, determined according to UNE EN 196-2 specifications, was around 46%. The obtained results are consistent with the study by Zanelli et al. [28] where, after analyzing 93 porcelain stoneware samples, they were composed mainly of an amorphous phase (40-80 wt-%) containing dispersed crystalline components, such as quartz (10-30 wt-%), mullite (4-10 wt-%) and feldespars (≈15 wt-%). As reported by García Ten [29], the amorphous phases in PS come about when sintering tiles (1190-1220ºC) due to the partial fusion of the crystalline phases. As explained by Li et al. [5], the term 'amorphous phase' is more appropriate for PS tiles than 'glassy' because, similarly to MK, the disordered phase is generated when breaking down the crystalline structure while sintering, which generally occurs at temperatures below those required to generate a liquid phase. In contrast, the glassy phase of GGBFS and fly ash is formed by melting and rapid cooling. However, as indicated in [5], although an amorphous structure is essential to reactivity, the amorphous content of the material and its hydraulic properties do not exactly correlate.

The mineralogical composition of PS was determined by X-ray diffraction in a Seifert diffractometer TT 3003 with Cu K_α radiation, 40 kV and 20 mA, 2θ from 5-55º. Quartz (SiO_2, PDFcard 331161) and mullite ($Al_6Si_2O_{13}$, PDFcard 150776) were the main phases identified in the raw material and, although feldspar phases were also expected [28], such as albite ($NaAlSi_3O_8$) or sanidine ($(K,Na)AlSi_3O_8$), they were not clearly identified by the XRD technique. Amorphous compounds were identified by the presence of a halo centered at 2θ = 15-30º.

2.2. Sample preparation

Pastes and mortars were prepared following the process described previously in [30]. The process variables used in this study are summarized in Table 1. As observed, the Na^+ concentration in the activating solution (provided by NaOH and sodium silicate) varied from 5.0 to 12.5 mol·kg^{-1}, while the

SiO_2 concentration ranged from 1.82 to 7.28 $mol.kg^{-1}$. The water/binder (w/b, the binder is the amount of ceramic waste) ratio was kept constant in all the samples (0.40) and variable amounts of $Ca(OH)_2$ (93% purity) were used to substitute ceramic waste (0-5% replacement). Pastes and mortars were cured in a thermostatically controlled bath at 65°C with relative humidity higher than 95%. A sand/binder ratio of 3:1 was used for all the prepared mortars.

Table 1. Process variables of the alkaline-activated porcelain stoneware

Variable	Range
w/b	0.40
Na^+, $mol.kg^{-1}$	2.5-12.5
SiO_2, $mol.kg^{-1}$	1.82-7.28
$Ca(OH)_2$, %Wt	0-5
Sand/binder	3:1

2.3. Pastes and mortars characterization

Alkali-activated PS mortars were prepared to evaluate the setting time and compressive strength. The pastes of the selected mortars were mixed to assess the evolution of the microstructure and reaction products during the alkali activation process. For this purpose, thermogravimetric analyses, microscopic studies, pH measurements, XRD tests and FTIR analyses were conducted.

The setting time was determined in mortars. For this purpose, a 5 kg load was applied on an area of 1 cm^2 every hour. The final setting time was that in which no appreciable trace was observed on the specimen surface.

The compressive strength of the mortar samples was tested following the UNE EN 196-1 specification. The dispersion from the mean values was taken as the standard deviation, which was the source of the error bars. Thermogravimetric analyses were performed in a TGA 850 Mettler-Toledo thermobalance at a heating rate of 10ºC min^{-1} from 35ºC to 600ºC using pin-holed aluminum crucibles. Microscopic studies were carried out by SEM using a JEOL-JSM-6300 equipped with an energy dispersive X-ray (EDX) for the microanalysis. pH values were determined by dissolving 1 g of paste with 10 ml of distilled water for 1 min. Measurements were taken on a micropH2001 by Crison. The FTIR (400 to 1500 cm^{-1}) of the PS and alkali-activated pastes were recorded in the transmittance mode on a Mattson Genesis II spectrometer with samples such as KBr pellets.

3. Results and Discussion

3.1. Setting time of the mortar samples containing 2% $Ca(OH)_2$

Previous studies have reported the strong influence of $Ca(OH)_2$ on the behavior of alkali-activated PS mortars [23]. Although calcium was required for the hardening process, contents higher than 5% resulted in rapid mortar setting. Granizo et al. [13] observed a similar behavior in 5M NaOH alkali-activated MK pastes, where no hardening occurred in the absence of $Ca(OH)_2$. Dombrowski et al. [16] also concluded that calcium acted as a reaction germ which, in a certain amount, quickened the reaction to more structure-forming products. According to Garcia-Lodeiro et al. [31], who analyzed the interaction between synthetic sodium aluminosilicate hydrate gels and aqueous Ca^{+2}, this element was taken in the N-A-S-H gels, and resulted in a modified chemical composition due to the substitution of sodium for calcium to form (N,C)-A-S-H gels. Furthermore, the scientific community [9,13,14,16] has proved that when adding calcium to the system, both C-S-H and sodium aluminosilicate hydrate (N-A-S-H) may coexist. According to Yip et al. [9], the C-S-H gel formed in such a system gave a significantly lower Ca/Si ratio than the C-S-H commonly formed from the hydration of Portland cement.

In order to understand the influence of calcium on the hardening process of alkali-activated PS, mortars with a constant 2% substitution of porcelain stoneware powder with $Ca(OH)_2$, variable Na^+ and SiO_2 concentrations were prepared. Figure 1 presents the setting time of these samples. Unexpectedly it varied vastly, ranging from a few minutes to 10 h, and two main groups were established according to the evolution of the setting time with sodium concentration. So while no correlation was observed in the samples mixed with low SiO_2 concentrations (1.82 and 3.64 SiO_2 mol/kg), the setting time of the mortars mixed with a larger amount of SiO_2 (5.46 and 7.28 mol/kg) increased linearly with the sodium concentration. Furthermore, while only the mortars with 5 mol/kg of Na^+ were successfully mixed with low SiO_2 contents, the setting time of the mortars mixed with higher SiO_2 concentrations was long enough to cast and vibrate samples properly.

This behavior, together with the fact that all the mortars with 5 mol/kg of sodium set in 4 h no matter what the SiO_2 concentration was, suggests that the setting time is linked to the $Ca(OH)_2$ to Na^+ ratio. The obtained results are consistent with those previously reported in [5,10-13], which proved that the

influence of $Ca(OH)_2$ depended on the activator concentration. As Na^+ is provided by both sodium silicate and NaOH, increasing amounts of sodium, and keeping the silicon concentration constant, imply higher OH^- concentrations (higher pH values). According to [5,10,12,13], calcium in a system at low alkalinity was dissolved from $Ca(OH)_2$ and took part in the formation of an C-S-H/C-(A)-S-H gel in preference to the formation of a calcium-based alkali-network structure, which usually forms more slowly than C-S-H under ideal conditions. Conversely, high OH^- concentrations hindered $Ca(OH)_2$ dissolution and, because the number of Ca^{2+} ions was insufficient to achieve saturation, the N-A-S-H gel became the predominant phase formed, together with small calcium precipitates scattered within the binder. Further studies conducted by Garcia-Lodeiro et al. [12] on synthetic samples have proved that, if sufficient calcium is provided, pH values of over 12 favor the formation of C-A-S-H gels rather than N-A-S-H gels.

3.2. Modulus of the mixes and their influence on the behavior of fresh mortars

Different ratios were set to analyze the fresh behavior of mixes (Table 2). While the modulus of solution (M_s) was defined as the SiO_2 to Na_2O mass ratio, the modulus of sodium (M_{Na}) related the moles of Na^+ in the activating solution to the SiO_2 and Al_2O_3 content in the raw material (PS). Finally, the modulus of calcium (M_{Ca}) showed a correlation between the moles of Ca^{2+} (to substitute the ceramic material, and after considering 93% purity) and the Na^+ moles in the activating solution.

Table 2. Ratios of mixes

Variable	Type	Range
M_s	Modulus of solution, mass	$\frac{SiO_{2\,SOLUTION}}{Na_2O_{SOLUTION}}$
M_{Na}	Modulus of sodium, molar	$\frac{Na^+{}_{SOLUTION}}{(SiO_2 + Al_2O_3)_{PS}}$
M_{Ca}	Modulus of calcium, molar	$\frac{Ca^{2+}{}_{HYDRATED\_LIME}}{Na^+{}_{SOLUTION}}$

The molar ratios and behavior of the fresh mortars mixed with 2% $Ca(OH)_2$ are reported in Table 3.

Table 3. Fresh behavior and ratios of the mortars mixed with 2% $Ca(OH)_2$

SiO_2, mol/kg	Na^+, mol/kg	M_S	M_{Na}	M_{Ca}	Fresh behavior / setting time, h
1.82	5.0	0.71	0.15	0.126	4
	7.5	0.47	0.22	0.084	Rapid setting
	10	0.35	0.30	0.063	Rapid setting
3.64	2.5	2.82	0.07	0.251	Non compactable
	5.0	1.41	0.15	0.126	4
	7.5	0.94	0.22	0.084	Rapid setting
	10	0.71	0.30	0.063	Rapid setting
5.46	3.0	3.53	0.09	0.209	Poor workability
	5.0	2.12	0.15	0.126	4
	7.5	1.41	0.22	0.084	7
	10	1.06	0.30	0.063	10
7.28	5	2.82	0.15	0.126	4
	7.5	1.88	0.22	0.084	7
	10	1.41	0.30	0.063	10

Mixes with an M_S higher than 2.5 and an M_{Na} lower than 0.1 (simultaneously) presented very poor workability. Although the workability of the mortar with an M_{Na} of 0.09 was quite poor, it was successfully placed into the mold and vibrated. However, it was not possible to compact the mortar mixed with an M_{Na} of 0.07 because dry particles formed during the vibration process, which hardened independently instead of binding the materials together. Moreover, rapid setting occurred in the mortars mixed with an M_S lower than 1 and an M_{Na} higher than 0.2. Both behaviors are summarized in Equations (1) and (2):

$$M_S<1 \wedge M_{Na}>0.2 \rightarrow \text{Rapid Setting} \quad (1)$$

$$M_S>2.5 \wedge M_{Na}<0.1 \rightarrow \text{Poor Workability} \quad (2)$$

In general terms, it can be stated that rapid setting occurred when too much sodium, related to the SiO_2 content (M_S<1), was added to the mix, while loss of workability was observed in the mixes to which not enough sodium was provided (M_S>2.5). This leads to the conclusion that in order to optimize the fresh behavior of alkali-activated PS mortars, it is highly recommendable to keep the M_S between 1 and 2.5 when designing mixes. This recommendation is consistent with the studies previously performed by Bernal et al. [14], where mixes with an M_S from 1.6 to 2.4 were designed for alkali-activated granulated blast furnace slag/metakaolin (GBFS/MK) blends. In [1], the modulus of the mixed alkali activator (the SiO_2/Na_2O molar ratio) was kept between 1.0 and 2.0. According to Provis et al. [32], although the optimum activator concentration depended on the precursor, this had to be the case for the charges of tetrahedral Si and Al to be balanced in order to avoid the presence of unreacted sodium or silica.

From the analyses of the proposed ratios it was also observed that when no rapid setting occurred, M_{Ca} governed the setting time, so it was equal for all the samples presenting the same Ca^{2+} to Na^+ molar ratio. In order to corroborate this influence, the amount of $Ca(OH)_2$ was adapted for the high silica-containing samples (5.46 and 7.28 mol/kg), and the mortars with a constant M_{Ca} modulus (0.126) were mixed (2, 3 and 4 wt-% of $Ca(OH)_2$ for the 5, 7.5 and 10 Na^+ concentrations, respectively). As expected, it was possible to demold all these mortars after curing for 4 h at 65ºC.

3.3. Compressive strength of mortar samples

The compressive strengths of the mortars prepared with variable SiO_2 and Na^+ concentrations, which were cured at 65ºC for 3 days, are depicted in Figure 2. The results of the mortars mixed with a constant amount of $Ca(OH)_2$ (2 wt-%) are plotted in Figure 2a, while those of the mortars mixed with increasing amounts of $Ca(OH)_2$ (constant M_{Ca} ratio) are reported in Figure 2b. Whereas the mortars with 2 wt-% $Ca(OH)_2$ exhibited a maximum compressive strength for a 7.5 mol/Kg sodium concentration, the compressive strength of the samples with a constant M_{Ca} modulus increased linearly up to the maximum Na^+ concentration (10 mol/kg). This behavior might be connected with the fact that higher OH^- concentrations may hinder the dissolution of $Ca(OH)_2$ by delaying the hardening process and gel formation (C-S-H/C-(A)-S-H/(N,C)-A-S-H). According to Yip et al. [10], C-S-H gel

formation in an alkali-activated binder is thought to work as a micro-aggregate in such a way that the resultant binder is homogeneous and dense, which increases mechanical strength.

For the mortars mixed with a constant M_{Ca}, the slope of the trend line was more pronounced in the mortars mixed with the highest SiO_2 concentration, which suggests a further increase in strength with additional Na^+ concentrations. This expected behavior was corroborated by designing a mortar with further sodium contents (12.5 mol/kg). Next 5% of $Ca(OH)_2$ was added to keep the setting time at 4 h (M_{Ca} = 0.126), and the calculated M_s and M_{Na} ratios were 1.13 and 0.38, respectively. The compressive strength of the mortars mixed with 7.28 moles per kg of SiO_2 and variable amounts of sodium, cured for 3 and 7 days at 65ºC, is shown in Figure 3. These results suggest that it may be a potential cementitious construction material, and they come close to the results reported previously in [30], where mortars with up to 42 MPa were obtained by the alkali activation of red hollow bricks (7 curing days at 65ºC). Similar values (40 MPa) were obtained by Guo et al. [1] in alkali-activated class C Fly ash pastes, cured at 75ºC for 24 h. Khater et al. [21], who also added calcium hydroxide to activate waste concrete and demolished walls, developed pastes with up to 23 MPa after curing at 40ºC for 90 days.

The results presented herein agree with those reported by Guo et al. [1], who pointed out that one of the most important variables that affects compressive strength is the M_S. As these authors explained, increasing alkali concentrations may improve compressive strength because the solubility of alumino-silicate present in the raw material increases, thus allowing the amorphous structure to partially or totally dissolve to be then transformed into a very compacted composite. In the present study, the M_S of the mortars showing the best compressive strengths ranged from 1.06 to 1.41. These values are close to those reported in [1], where the best compressive strength results in alkali-activated class C Fly ash pastes, cured at both room temperature and high temperature, were obtained with an M_S of 1.5. Although Bernal et al. [14] observed relatively low performance in the GBFS mortars activated with an Ms of 1.60, these authors attributed this behavior to a low degree of binder formation due to a very short setting time.

3.4. Characterization of pastes mixed with a constant 7.28 mol/Kg SiO_2 concentration

The pastes mixed with 7.28 moles of SiO_2 per kg of activating solution and variable concentrations of sodium and $Ca(OH)_2$ were prepared to investigate the evolution of the alkali activation process. They were cured at 65ºC for 7 days.

3.4.1. pH measurements

pH values were determined in the pastes cured at 65ºC up to 7 days (Fig. 4). The values were higher than 11.6 for all the pastes developed and, as expected, they were higher for increasing sodium concentrations, but they lowered with curing time. A reduction in pH with curing time is associated with the formation of reaction products during the alkali activation process. These results corroborate the influence of M_{Ca} on the hardening process since more calcium was required in the mixes with higher pH values to keep the setting time constant. As observed by Li et al. [5], this is due to the solubility of calcium decreases with pH.

3.4.2. Scanning electron microscopy

The SEM micrographs of the pastes mixed with 5.0 to 12.5 moles of sodium per kg of activating solution, cured for 7 days at 65ºC, are depicted in Figure 5. As observed, the microstructure becomes denser with addition of sodium, which is in good agreement with the evolution of the mechanical properties.

Sodium-calcium carbonates were observed in the samples with 5.0 and 7.5 mol/kg of sodium (micrographs 5a and 5b, respectively). Presence of these salts was corroborated by XRD analyses (see Section 3.4.3).

3.4.3. X-ray diffraction (XRD) studies

Figure 6 shows the XRD patterns of the PS raw material and the pastes mixed with 7.28 SiO_2 mol/kg and increasing amounts of sodium, cured for 7 days at 65ºC. The main crystalline phases identified in the raw material (quartz,Q, PDFcard 331161; and mullite, M, PDFcard 150776) persisted after the activation process, which indicates that they reacted only partially or did not react at all. The hump in

the raw material (2θ = 15-30º) displaced toward higher diffraction angles (2θ = 20-40º) after the activation process (see Fig. 6b). This shift became more pronounced for higher sodium contents, which is consistent with the compressive strength evolution presented by mortars. As reported by Guo et al. [1], this hump is characteristic of amorphous gels, which include not only the aluminosilicate gel formed during the alkali activation process, but also the calcium silicate hydrate (C–(A)-S–H) gel. The presence of sodium-calcium carbonates, previously identified by SEM, was corroborated by XRD. Minor quantities of natrite (N, Na_2CO_3, PDFcard 370451) and calcite (C, $CaCO_3$, PDFcard 050586) were identified in the alkali-activated pastes with increasing amounts of added sodium. In fact, they were only clearly distinguished later by FTIR analyses in pastes mixed with the highest sodium contents (12.5 sodium mol/kg).

No new crystalline peaks were observed after the activation process, which leads to the conclusion that neither crystalline C-(A)-S-H nor zeolite type reaction products were dominant after the alkaline activation of PS under our research conditions. Although the work by Dombrowsky et al. [16] detected crystalline C–S–H phases (reinhardtsbraunsite), the amount of $Ca(OH)_2$ initially present in the samples (20%) was significantly higher than that used in the present study. Finally, despite some crystalline zeolite-type reaction products, such as gismondine, sodalite, Na-Herschelite or hydroxysodalite, having been found to be secondary reaction products in [1,8,14,16], it was not possible to clearly identify them in the PS alkali-activated pastes. This finding is in agreement with the study by Duxson et al. [33], who indicated that the formation of zeolitic phases in highly concentrated solutions was not likely to be due to phase transport and reorganization difficulties.

3.4.4. Thermogravimetric analysis

The differential thermogravimetric curves and the total weight loss of the PS pastes mixed with 7.28 SiO_2 mol/kg and variable Na^+ concentrations, cured at 65ºC for 7 days, are depicted in Figure 7. A single peak, centered at approximately 130ºC, was observed in all the mixes, and it is related to water loss by the dehydration of gels. Consistently with the data reported by Bernal et al. [14], greater water loss with increasing sodium concentration was observed, which may be associated with the presence of more chemically-bound water.

No signals associated with the zeolitic-type reaction products were distinguished by the TG analyses as they tend to show a dehydration peak within the 60-160ºC temperature range [14]. In agreement with the XRD results, no peaks associated with the decomposition of $Ca(OH)_2$ appeared (500-600ºC), which means that this reagent was totally consumed during matrix formation. No signals associated with the dehydration of the C-S-H gel (≈380ºC) [14] were identified. This suggests that, due to the small amount of $Ca(OH)_2$ available in the system and the high alkalinity of the medium, the N-A-S-H gel was the predominant phase formed, and that calcium was taken within it to form (N,C)-A-S-H gels.

3.4.5. Fourier-transformed infrared spectroscopy (FTIR) studies

The FTIR spectra of the PS and alkali-activated pastes mixed with 7.28 SiO_2 mol/kg and variable Na^+ concentrations, cured at 65ºC for 7 days, are shown in Figure 8. Presence of quartz (1145, 1084, 796–778, 697, 668, 522 and 460 cm^{-1}) and mullite (1185 cm^{-1} [34]), as previously detected by XRD, was corroborated by FTIR. They were observed in both PS raw material and alkali-activated pastes, which confirms that they barely altered during the alkali activation process.

Signals from different compounds overlapped in the broad band and appeared from 900 cm^{-1} to 1250 cm^{-1}. Similarly to other ceramic products, such as red clay ceramic waste [30], the main band in the unreacted PS appeared at ~1071 cm^{-1} and, according to Criado et al. [34], it was associated with the amorphous phases in raw material. After the alkali activation process, this band shifted to lower wave numbers (1020 and 1013 cm^{-1}), which is attributed to the asymmetric stretching vibrations generated by the T–O–T bonds (T: Si or Al) in the newly formed N-A-S-H gel [31]. As observed by Criado et al. [34], early in the reaction, an Al-enriched gel was formed, and the Al-O bonds were weaker and more readily broken than the Si-O bonds. As the reaction progressed, the silica content in the gel gradually increased, giving rise to a Si-rich gel, and this was responsible for the mechanical properties of the material. Richer silicon gels were reflected in the IR spectra by a shift of the main band toward higher frequencies, suggesting that the Si/Al ratio of the formed gel was slightly lower in the pastes mixed with 10 and 12.5 mol/kg of sodium. However, as these mixes presented a denser microstructure and better mechanical properties, the influence of calcium must also be considered. Although the exact role of calcium in the reaction process did not come over clearly, several studies suggest that it may participate in calcium silicate hydrate (C-(A)–S–H) gel formation, or that it might act as a charge-

balancing ion, which would lead to (C,N)–A–S–H gels [1,16,31]. In the study by Guo et al. [1], calcium was found to act in both ways and, while the main reaction products of alkali-activated class C fly ash were seen to coexist with the calcium silicate hydrate (C– S–H) gel, calcium also provided a charge balance during the alkali activation process. According to Garcia-Lodeiro et al. [31], the displacement of sodium by calcium in the (C,N)-A-S-H gels did not imply relevant changes in the position of the bands, no matter what the initial Ca/Si ratio of the mix was. Dombrowsky et al. [16] also observed that both the aluminosilicate gels and C–S–H-phases coexisted when replacing fly ash with calcium hydroxide (0-20%). In that study, proportions of formed C-S-H varied in accordance with the alkaline activator concentration, and they were especially high in the samples with the highest calcium content, which also contained zeolitic phases. In the alkali-activated PS pastes, no bands were observed between 660 and 720 cm^{-1}, as pointed out by Rees et al. [35] and Granizo et al. [13] as being zeolite-characteristic.

Although sodium-carbonate salts were identified by the SEM and XRD, the signals associated with these phases were noticeable only for the 12.5 sodium mol/kg paste. Their presence has been associated with the low-intensity band appearing at wave numbers higher than 1400 cm^{-1} as, according to Zaki et al. [36], CO_2 impurity species shift the band associated with pure $CaCO_3$ (1415 cm^{-1} [37]) to higher wave numbers.

4. Conclusions

Porcelain stoneware has been activated by alkali solutions. The activator concentration and calcium hydroxide addition strongly influence the fresh behavior of mortars in such a way that, in order to achieve good workability and to avoid rapid setting, the modulus of solution (SiO_2/Na_2O) should be kept at between 1 and 2.5 when designing alkali-activated PS mixes. The calcium to sodium molar ratio (M_{Ca}) greatly influences the hardening process, while the mortars mixed with a constant M_{Ca} present an equal setting time. Compressive strength increases linearly with sodium concentration when keeping both the M_{Ca} and silica concentration in the activator constant, and mortars with up to 36 MPa can be obtained after 7 days of curing at 65°C. While the formation of amorphous gels has been confirmed by the microstructural analysis, neither $Ca(OH)_2$ nor new crystalline phases was/were observed after the alkali activation process.

Acknowledgements

The authors are grateful to the Spanish Ministry of Science and Innovation for supporting this study through Project GEOCEDEM BIA 2011-26947, and to FEDER funding.

References

[1] Guo X, Shi H, Dick WA. Compressive strength and microstructural characteristics of class C fly ash geopolymer. Cement Concrete Comp 2010;32:142–147.

[2] He J, Jie Y, Zhang J, Yu Y, Zhang G. Synthesis and characterization of red mud and rice husk ash-based geopolymer composites. Cement Concrete Comp 2013;37:108–118.

[3] Shi C, Fernández Jiménez A, Palomo A. New cements for the 21st century: The pursuit of an alternative to Portland cement. Cement Concrete Res 2011;41:750–763.

[4] Payá J, Borrachero MV, Monzó J, Soriano L, Tashima MM. A new geopolymeric binder from hydrated-carbonated cement. Mater Lett 2012;74:223-225.

[5] Li C, Sun H, Li L. A review: The comparison between alkali-activated slag (Si+Ca) and metakaolin (Si+Al) cements. Cement Concrete Res 2010;40:1341–1349.

[6] Van Deventer JSJ, Provis JL, Duxson P, Brice DG. Chemical research and climate change as drivers in the commercial adoption of alkali activated materials. Waste Biomass Valor 2010;1:145–155.

[7] Alonso S, Palomo A. Alkaline activation of metakaolin and calcium hydroxide mixtures: influence of temperature, activator concentration and solids ratio. Mater Lett 2001;47:55–62.

[8] Fernández-Jiménez A, de la Torre AG, Palomo A, López-Olmo G, Alonso MM, Aranda MAG. Quantitative determination of phases in the alkaline activation of fly ash. Part II: Degree of reaction. Fuel 2006;85:1960–1969.

[9] Yip CK, van Deventer JSJ. Microanalysis of calcium silicate hydrate gel formed within a geopolymeric binder. J Mater Sci 2003;38:3851 – 3860.

[10] Yip CK, Lukey GC, van Deventer JSJ. The coexistence of geopolymeric gel and calcium silicate hydrate at the early stage of alkaline activation. Cement Concrete Res 2005;35:1688– 1697.

[11] García-Lodeiro I, Palomo A, Fernández-Jiménez A, Macphee DE. Compatibility studies between N-A-S-H and C-A-S-H gels. Study in the ternary diagram Na_2O-CaO-Al_2O_3-SiO_2-H_2O. Cement Concrete Res 2011;41:923–931.

[12] García-Lodeiro I, Maltseva O, Palomo A, Fernández-Jiménez A. Hybrid alkaline cements. Part I: Fundamentals. Rev Rom Mater 2012;42 (4):330–335.

[13] Granizo ML, Alonso S, Blanco-Varela MT, Palomo A. Alkaline Activation of Metakaolin: Effect of Calcium Hydroxide in the Products of Reaction. J Am Ceram Soc 2002;85 (1):225–31.

[14] Bernal SA, Gutierrez RM, Provis JL, Rose V. Effect of silicate modulus and metakaolin incorporation on the carbonation of alkali silicate-activated slags. Cement Concrete Res 2010;40:898–907.

[15] Jang JG, Lee NK, Lee HK. Fresh and hardened properties of alkali-activated fly ash/slag pastes with superplasticizers. Constr Build Mater 2014;50:169–176.

[16] Dombrowski K, Buchwald A, Weil M. The influence of calcium content on the structure and thermal performance of fly ash based geopolymers. J Mater Sci 2007;42:3033–3043.

[17] Lee NK, Kim HK, Park IS, Lee HK. Alkali-activated, cementless, controlled low-strength materials (CLSM) utilizing industrial by-products. Constr Build Mater 2013;49:738–746.

[18] Yusuf MO, Johari MAM, Ahmad ZA, Maslehuddin M. Strength and microstructure of alkali-activated binary blended binder containing palm oil fuel ash and ground blast-furnace slag. Constr Build Mater 2014;52:504–510.

[19] Kourti I, Rani DA, Deegan D, Boccaccini AR, Cheeseman CR. Production of geopolymers using glass produced from DC plasma treatment of air pollution control (APC) residues. J Hazard Mater 2010;176:704–709.

[20] Sun Z, Cui H, An H, Tao D, Xu Y, Zhai J, Li Q. Synthesis and thermal behavior of geopolymer-type material from waste ceramic. Constr Build Mater 2013;49:281–287.

[21] Khater HM. Effect of Calcium on Geopolymerization of Aluminosilicate Wastes. J Mater Civ Eng 2012;24 (1):92–101.

[22] Puertas F, García-Díaz I, Barba A, Gazulla MF, Palacios M, Gómez MP, Martínez-Ramírez S. Ceramic wastes as alternative raw materials for Portland cement clinker production. Cement Concrete Comp 2008;30 (9):798-805.

[23] Reig L, Tashima MM, Soriano L, Borrachero MV, Monzó J, Payá J. Alkaline Activation of Ceramic Waste Materials. Waste Biomass Valor. http://dx.doi.org/10.1007/s12649-013-9197-z.

[24] Stock D. World production and consumption of ceramic tiles. Tile Today 2011;73:50–58.

[25] Puertas F, Barba A, Gazulla MF, Gómez MP, Palacios M, Martínez-Ramírez S. Residuos cerámicos para su posible uso como materia prima en la fabricación de clínker de cemento Portland: caracterización y activación alcalina. Mater Construcc 2006;56 (281):73-84.

[26] Pereira-de-Oliveira LA, Castro-Gomes JP, Santos PMS. The potential pozzolanic activity of glass and red-clay ceramic waste as cement mortars components. Constr Build Mater 2012;31:197-203.

[27] Medina C, Juan A, Frías M, Sánchez-de-Rojas MI, Morán JM, Guerra MI. Characterization of Concrete made with Recycled Aggregate from Ceramic Sanitary Ware. Mater Construcc. 2011;61 (304):533-546.

[28] Zanelli C, Raimondo M, Guarini G, Dondi M. The vitreous phase of porcelain stoneware: Composition, evolution during sintering and physical properties. J Non-Cryst Solids 2011;357:3251–3260.

[29] García Ten F.J. Descomposición durante la cocción del carbonato cálcico contenido en el soporte crudo de los azulejos. Tesis de doctorado, Departamento de Ingeniería química, UJI; 2005.

[30] Reig L, Tashima MM, Borrachero MV, Monzó J, Cheeseman CR, Payá J. Properties and microstructure of alkali-activated red clay brick waste. Constr Build Mater 2013;43:98–106.

[31] García-Lodeiro I, Fernández-Jiménez A, Palomo A, Macphee DE. Effect of Calcium Additions on N–A–S–H Cementitious Gels. J Am Ceram Soc 2010;93 (7):1934–1940.

[32] Provis JL, Harrex RM, Bernal AS, Duxson P, van Deventer JSJ. Dilatometry of geopolymers as a means of selecting desirable fly ash sources. J Non-Cryst Solids 2012;358:1930–1937.

[33] Duxson P, Fernández-Jiménez A, Provis JL, Lukey GC, Palomo A, van Deventer JSJ. Geopolymer technology: the current state of the art. J Mater Sci 2007;42 (9):2917–93.

[34] Criado M, Fernández-Jiménez A, Palomo A. Alkali activation of fly ash: effect of the SiO_2/Na_2O ratio Part I: FTIR study. Micropor Mesopor Mater 2007;106:180–91.

[35] Rees CA, Provis JL, Lukey GC, van Deventer JSJ. Attenuated total reflectance fourier transform infrared analysis of fly ash geopolymer gel aging. Langmuir 2007;23:8170–9.

[36] Zaki MI, Knözinger H, Tesche B, Mekhemer GAH. Influence of phosphonation and phosphation on surface acid-base and morphological properties of CaO as investigated by in situ FTIR spectroscopy and electron microscopy. J Colloid Interface Sci 2006;303:9–17.

[37] Tatzber M, Stemmer M, Spiegel H, Katzlberger C, Haberhauer G, Gerzabek MH. An alternative method to measure carbonate in soils by FTIR spectroscopy. Environ Chem Lett 2007;5:9–12.

LIST OF FIGURES:

Fig. 1. Setting time of the mortars mixed with 2% $Ca(OH)_2$ and different Na^+ and SiO_2 concentrations

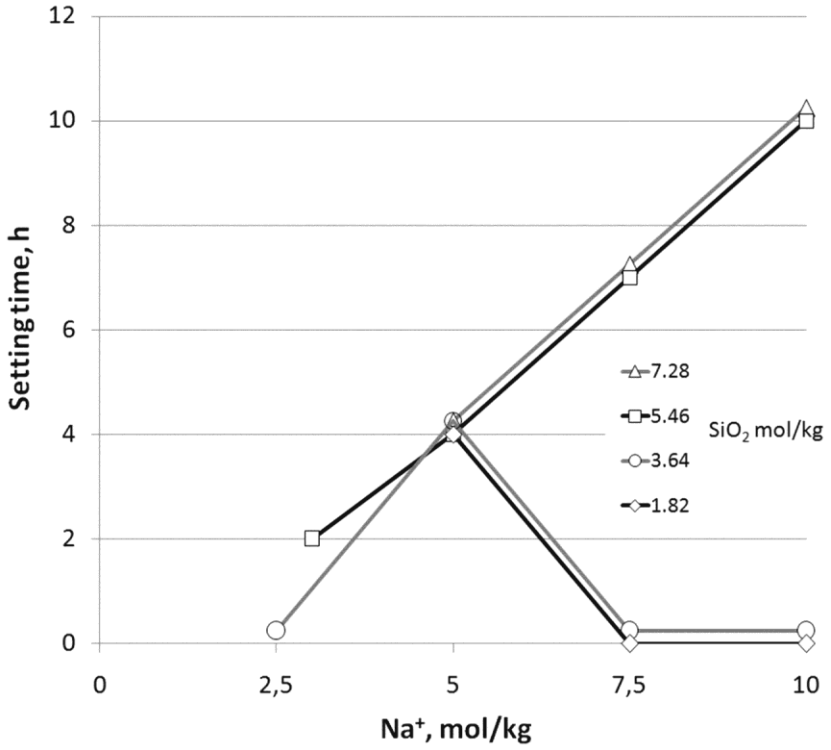

Fig. 2. Compressive strength of the mortars mixed with variable SiO_2 and Na^+ concentrations: a) Constant 2% $Ca(OH)_2$ in substitution; b) Variable percentages of $Ca(OH)_2$ in substitution

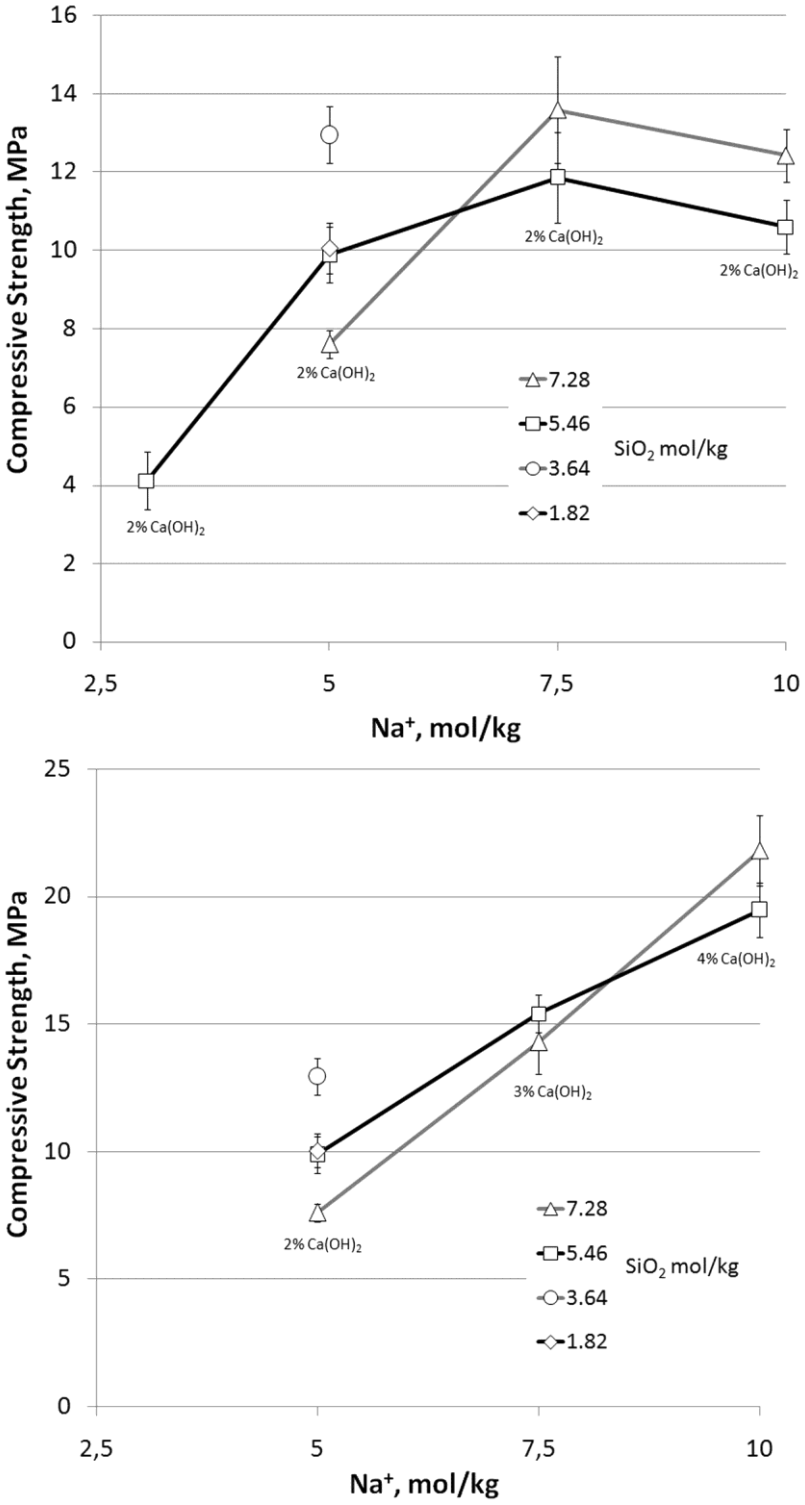

Fig. 3. Compressive strength of the mortars mixed with 7.28 SiO_2 mol/kg and variable Na^+ concentrations, cured for 3 and 7 days at 65ºC

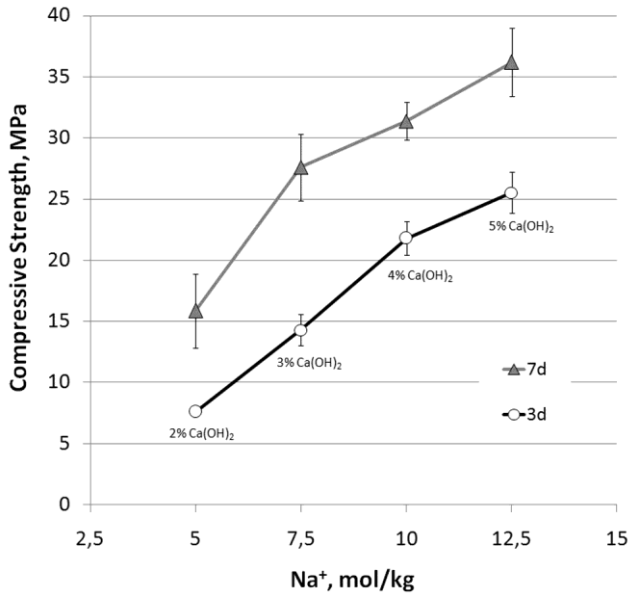

Fig. 4. pH values of the PS pastes mixed with 7.28 SiO_2 mol/kg and variable Na^+ concentrations, cured at 65ºC up to 7 days

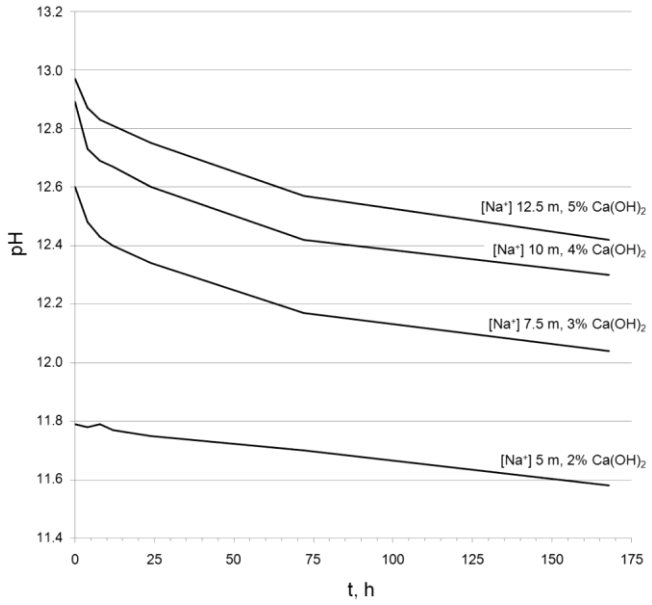

Fig. 5. Scanning electron microscope images of the PS alkali-activated pastes, mixed with 7.28 SiO2 mol/kg and variable Na^+ concentrations, cured for 7 days at 65ºC: a) Na^+ 5 mol/kg, 2% $Ca(OH)_2$; b) Na^+ 7.5 mol/kg, 3% $Ca(OH)_2$; c) Na^+ 10 mol/kg, 4% $Ca(OH)_2$; d) Na^+ 12.5 mol/kg, 5% $Ca(OH)_2$

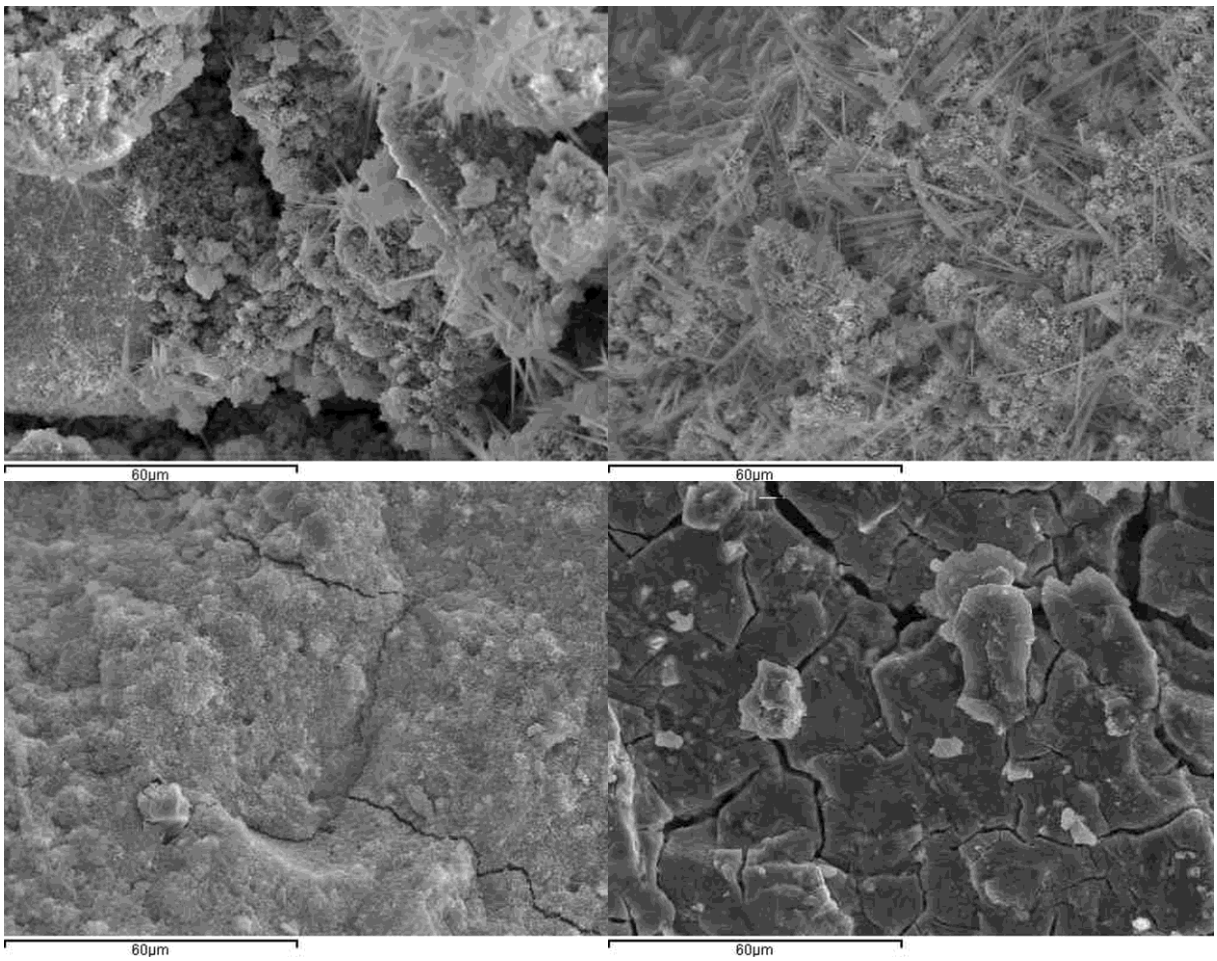

Fig. 6. X-ray diffractograms of raw material and alkali-activated pastes after curing at 65ºC for 7 days: Q quartz, M mullite, N natrite, C calcite: a) general view; b) magnification of the 15 to 40 2θ degree area.

1

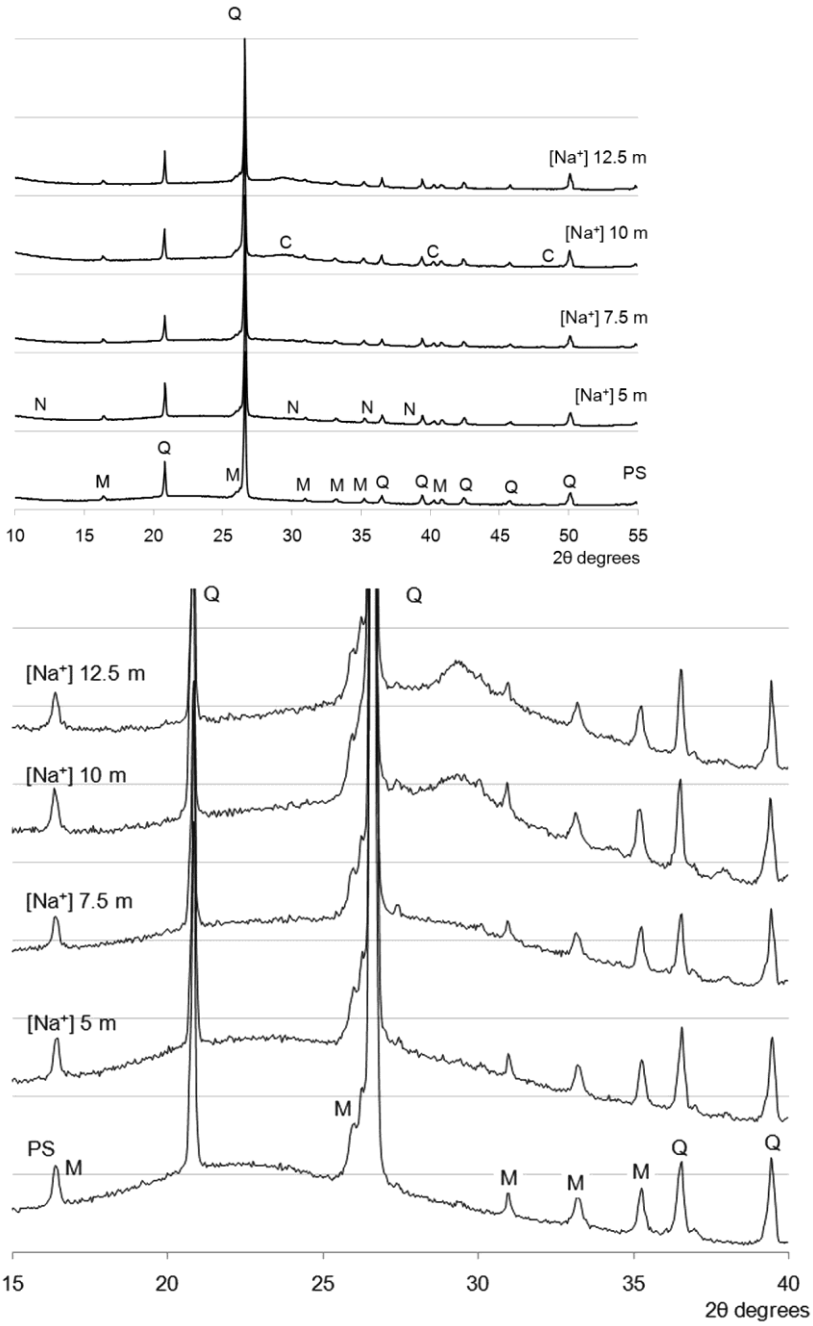

2

3 Fig. 7. Differential thermogravimetric curves and total weight loss of the PS pastes mixed with 7.28

4 SiO_2 mol/kg and variable Na^+ concentrations, cured at 65ºC for 7 days

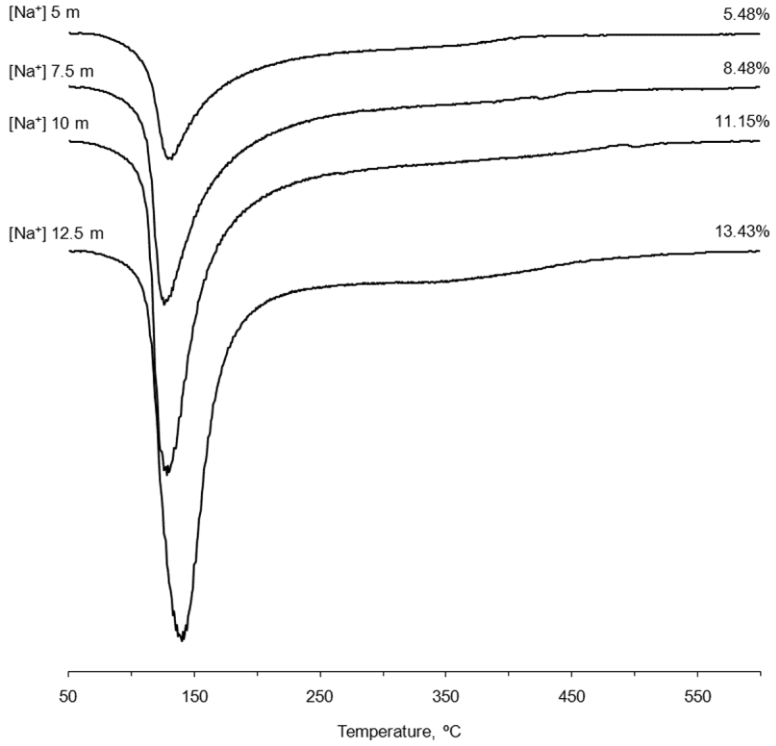

Fig. 8. FTIR spectra of the PS and alkali-activated pastes mixed with 7.28 SiO_2 mol/kg and variable Na^+ concentrations, cured at 65ºC for 7 days